

Standard and Non-Standard Physics in Neutrino Oscillations

M. Maltoni^a

^aInstituto de Física Corpuscular – CSIC/UVEG,
Edificio Institutos de Paterna, Apt. 22085, E-46071 Valencia, Spain

We analyze the impact of recent solar and atmospheric data in the determination of the neutrino oscillation parameters, taking into account that both the solar ν_e and the atmospheric ν_μ may convert to a mixture of active and sterile neutrinos. Furthermore, in the context of the atmospheric neutrino problem we discuss an extended mechanism of neutrino propagation which combines both oscillations and non-standard neutrino-matter interactions. We use the most recent neutrino data, including the 1496-day Super-K solar and atmospheric data samples, the latest SNO spectral and day/night solar data, and the final MACRO atmospheric results. We confirm the clear preference of all the data for pure-active oscillation solutions, bounding the fraction of sterile neutrino involved in oscillations to be less than 52% in the solar sector and less than 40% in the atmospheric sector, at 3σ . For the atmospheric case we also derive a bound on the total amount of non-standard neutrino-matter interactions, bounding the flavor-changing component to $-0.03 \leq \varepsilon \leq 0.02$ and the non-universal component to $|\varepsilon'| \leq 0.05$.

1. Introduction

The experimental data on atmospheric neutrinos [1,2] show, in the muon-type events, a clear deficit which cannot be accounted for without invoking non-standard neutrino physics. In addition to this, the recent results from the Sudbury Neutrino Observatory (SNO) on neutral current (NC) events [3] have added more weight to the already robust evidence that an extension of the Standard Model of particle physics is necessary in the leptonic sector. Altogether, the most popular explanation of both the solar and the atmospheric neutrino problem is provided by the neutrino oscillation hypothesis. However, many alternative attempts to account for neutrino anomalies without oscillations have recently been proposed [4]. While the results of solar neutrino experiments still admit very good alternative explanations [5], the atmospheric neutrino anomaly is so well reproduced by the $\nu_\mu \rightarrow \nu_\tau$ oscillation hypothesis [1,6] that one can use the robustness of this interpretation to place stringent limits on a number of alternative mechanisms [7].

In the present work we present an updated analysis of the solar and atmospheric neutrino data, first in the context of the standard oscillation hypothesis (Secs. 2 and 3), and then as-

suming that neutrino possesses also non-standard interactions with matter (Sec. 4). Motivated by the stringent limits from reactor experiments [8], we adopt an effective two-neutrino approach in which solar and atmospheric analyses decouple. However, in the pure-oscillation case presented in Secs. 2 and 3 our effective two-neutrino oscillation approach is generalized in the sense that it takes into account that a light sterile neutrino, advocated to account for the LSND anomaly [9], may participate in the conversion process [10]. The natural setting for such a light sterile neutrino is provided by four-neutrino models. In this paper we will determine the constraints on the oscillation parameters in this generalized scenario following from solar and atmospheric data *separately*, addressing the reader to our recent papers in Refs. [11,12] for a mass-scheme-dependent combined analysis of all current oscillation data.

2. Solar neutrino oscillations

In the following we analyze solar neutrino data in the general framework of mixed active-sterile neutrino oscillations. In this case the electron neutrino produced in the sun converts into a combination of an active non-electron neutrino ν_a (which again is a combination of ν_μ and ν_τ) and

Region	Active ($\eta_s = 0$)				Sterile ($\eta_s = 1$)			
	$\tan^2 \theta_{\text{SOL}}$	Δm_{SOL}^2	χ_{SOL}^2	GOF	$\tan^2 \theta_{\text{SOL}}$	Δm_{SOL}^2	χ_{SOL}^2	GOF
LMA	0.44	6.6×10^{-5}	66.1	85%	0.38	1.5×10^{-4}	99.0	6%
LOW	0.66	7.9×10^{-8}	75.1	60%	1.7	1.1×10^{-9}	102.0	4%
VAC	1.7	6.3×10^{-10}	75.0	61%	0.19	2.6×10^{-10}	89.0	21%
SMA	1.3×10^{-3}	5.2×10^{-6}	89.3	20%	3.6×10^{-4}	3.5×10^{-6}	99.4	6%
Just-So ²	1.0	5.5×10^{-12}	97.0	8%	1.0	5.5×10^{-12}	97.5	8%

Table 1

Best fit values of Δm_{SOL}^2 and θ_{SOL} , with the corresponding χ_{SOL}^2 and the GOF for $81 - 2$ d.o.f., for pure-active and pure-sterile solar neutrino oscillations.

a sterile neutrino ν_s :

$$\nu_e \rightarrow \sqrt{1 - \eta_s} \nu_a + \sqrt{\eta_s} \nu_s. \quad (1)$$

The parameter η_s with $0 \leq \eta_s \leq 1$ describes the fraction of the sterile neutrino participating in the solar oscillations. Therefore, the oscillation probabilities depend on the three parameters Δm_{SOL}^2 , θ_{SOL} and η_s .

As experimental data, we use the solar neutrino rates of the chlorine experiment Homestake [13], the most recent result of the gallium experiments SAGE [14] and GALLEX/GNO [15], as well as the 1496-days Super-Kamiokande data sample [16] in the form of 44 bins and the latest results from SNO presented in Ref. [3], in the form of 34 data bins. Therefore, we have a total of $3 + 44 + 34 = 81$ observables, which we fit in terms of the three parameters Δm_{SOL}^2 , θ_{SOL} and η_s . Further details about our statistical analysis can be found in [10].

We have performed a global fit of solar neutrino data, whose results are summarized in Tab. 1 and Fig. 1. Our global best fit point occurs in the LMA region, for $\tan^2 \theta_{\text{SOL}} = 0.44$, $\Delta m_{\text{SOL}}^2 = 6.6 \times 10^{-5} \text{ eV}^2$ and $\eta_s = 0$. We obtain a $\chi_{\text{min}}^2 = 66.1$, which for $81 - 3$ d.o.f. leads to an excellent goodness of fit of 83%. From Fig. 1 we can derive the 3σ bounds $0.25 \leq \tan^2 \theta_{\text{SOL}} \leq 0.83$, $2.6 \times 10^{-5} \text{ eV}^2 \leq \Delta m_{\text{SOL}}^2 \leq 3.3 \times 10^{-4} \text{ eV}^2$ and $\eta_s \leq 0.52$. Note that maximal mixing $\theta_{\text{SOL}} = 45^\circ$ is now ruled out, and that the upper bound on Δm_{SOL}^2 is rather solid even without the inclusion of reactor experiments [8].

From Tab. 1 we notice the strong discrimination against non-LMA solutions implied by the present data: in the pure-active case we find

$\Delta\chi_{\text{LOW}}^2 = 9.0$, $\Delta\chi_{\text{VAC}}^2 = 8.9$, $\Delta\chi_{\text{SMA}}^2 = 23.2$ and $\Delta\chi_{\text{Just-So}^2}^2 = 30.9$ relative to the global best fit in the LMA region. This shows that the first hints in favor of a globally preferred LMA oscillation solution, which followed mainly from the flatness of the Super-K spectra, have now become a robust result, thanks to the additional data to which SNO has contributed significantly. Note that especially SMA and Just-So² are highly disfavored with respect to LMA.

The inclusion of a sterile neutrino participating in the oscillation process is strongly disfavored by the solar data. From the right panel of Fig. 1 we first see how the preferred LMA solution survives in the presence of a *small* sterile component characterized by η_s . However, increasing η_s leads to a clear deterioration of all the oscillation solutions. Notice that there is a crossing between the LMA and VAC solutions, as a result of which the best pure-sterile description lies in the vacuum regime. However, in the global analysis sterile oscillations with $\eta_s = 1$ are highly disfavored. We find a χ^2 -difference between pure-active and pure-sterile of 32.9 in the LMA region, which decreases to 22.9 if we allow also for VAC. This means that pure-sterile oscillations are ruled out at 4.8σ compared to the active case.

In summary, we have found that, as long as the admixture of sterile neutrinos is acceptably small, the LMA is always the best of the oscillation solutions, establishing its robustness also in our generalized oscillation scheme.

3. Atmospheric neutrino oscillations

In our analysis of atmospheric data we make use of the hierarchy $\Delta m_{\text{SOL}}^2 \ll \Delta m_{\text{ATM}}^2$ and neglect

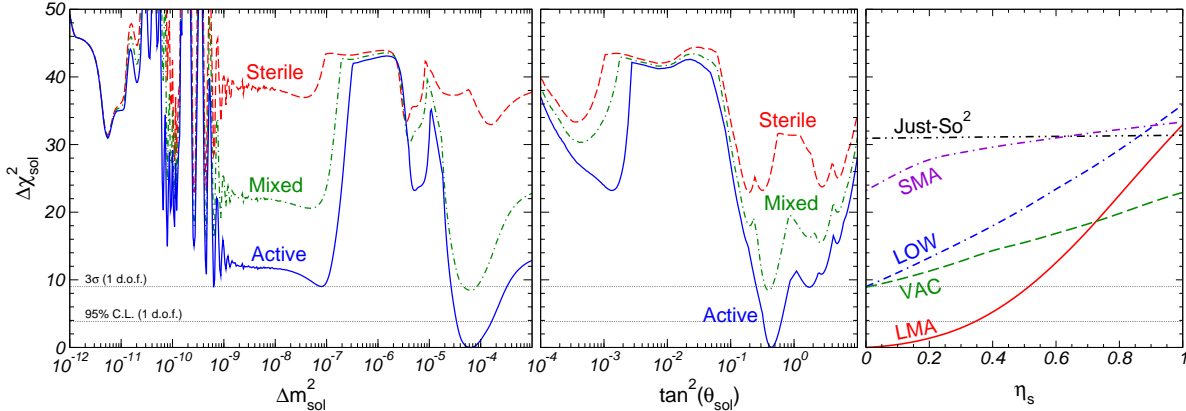


Figure 1. $\Delta\chi^2_{\text{SOL}}$ as a function of Δm^2_{SOL} , $\tan^2 \theta_{\text{SOL}}$ and η_s . In each panel the undisplayed parameters are integrated out. The “Active”, “Mixed” and “Sterile” labels correspond to $\eta_s = 0, 0.5$ and 1 , respectively.

the solar mass splitting [6]. Further, in order to comply with the strong constraints from reactor experiments [8] we completely decouple the electron neutrino from atmospheric oscillations [17]. In the following we consider a generalized oscillation scheme in which a light sterile neutrino takes part in the oscillations [10]. Such a scenario requires two more parameters in addition to θ_{ATM} and Δm^2_{ATM} . We use the parameters d_μ and d_s already introduced in Ref. [11], and defined in such a way that $(1 - d_\mu)$ and $(1 - d_s)$ correspond to the fractions of ν_μ and ν_s participating in oscillations with Δm^2_{ATM} , respectively. Hence, pure-active atmospheric oscillations are recovered in the limit $d_\mu = 0$ and $d_s = 1$.

In addition, we also present a “restricted” analysis in which the ν_μ is completely constrained to the atmospheric mass states, so that $d_\mu = 0$. In this limit the parameter d_s has a similar interpretation as η_s introduced in the solar case, and ν_μ oscillates into a linear combination of ν_τ and ν_s :

$$d_\mu = 0 : \quad \nu_\mu \rightarrow \sqrt{d_s} \nu_\tau + \sqrt{1 - d_s} \nu_s. \quad (2)$$

For the atmospheric data analysis we use all the charged-current data from the Super Kamiokande [1] and MACRO [2] experiments. The Super-Kamiokande data include the e -like and μ -like data samples of sub- and multi-GeV contained events (10 bins in zenith angle), as well as the stopping (5 angular bins) and through-going (10 angular bins) up-going muon data

events. From MACRO we use the through-going muon sample divided in 10 angular bins [2]. Therefore, we have 65 observables, which we fit in terms of the four parameters Δm^2_{ATM} , θ_{ATM} , d_μ and d_s . Further details can be found in Ref. [10].

The results of our analysis are summarized in Fig. 2. In contrast to the solar case, the atmospheric χ^2 exhibits a beautiful quadratic behavior, reflecting the high quality of the fit and the robustness of the oscillation solution. The global best fit point occurs at $\sin^2 \theta_{\text{ATM}} = 0.49$, $\Delta m^2_{\text{ATM}} = 2.1 \times 10^{-3} \text{ eV}^2$, $d_s = 0.92$ and $d_\mu = 0.04$, and exhibits a small but non-vanishing sterile neutrino component. However, this effect is not statistically significant, since also the pure-active case with $d_s = 1$ and $d_\mu = 0$ gives an excellent fit: for $\sin^2 \theta_{\text{ATM}} = 0.5$ and $\Delta m^2_{\text{ATM}} = 2.5 \times 10^{-3} \text{ eV}^2$, we have that the χ^2 -difference with respect to the best fit point is only 3.3.

From Fig. 2 we can extract the 3σ allowed ranges: $0.29 \leq \sin^2 \theta_{\text{ATM}} \leq 0.71$ and $9.2 \times 10^{-4} \text{ eV}^2 \leq \Delta m^2_{\text{ATM}} \leq 4.6 \times 10^{-3} \text{ eV}^2$ for the standard two-neutrino oscillation parameters, while for d_s and d_μ we have $(1 - d_s) \leq 0.40$ and $(1 - d_\mu) \geq 0.85$. So we see that atmospheric data essentially reject a sterile neutrino component, and strongly bound the ν_μ -content in atmospheric oscillations to be nearly maximal. Note that if we impose the condition $d_\mu = 0$, the 3σ limit on the sterile neutrino fraction improves to $(1 - d_s) \leq 0.19$.

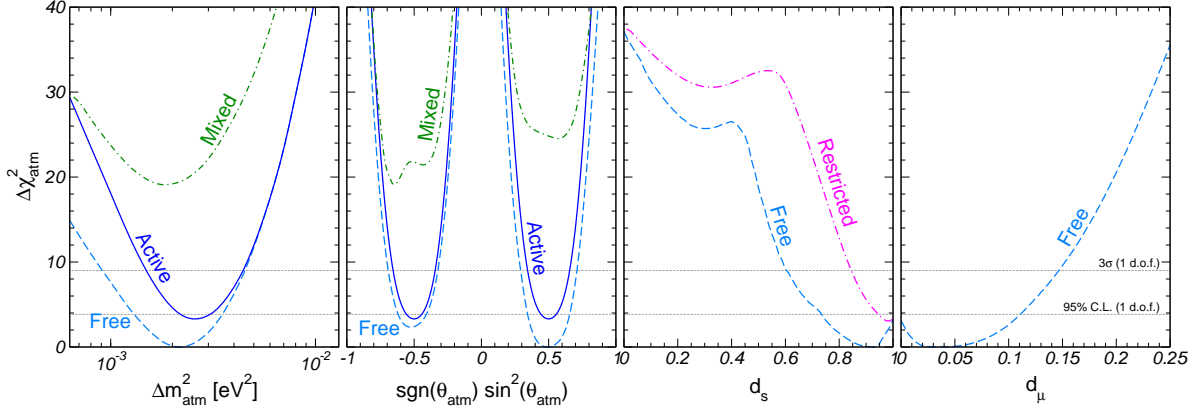


Figure 2. $\Delta\chi^2_{\text{atm}}$ as a function of Δm^2_{atm} , $\sin^2\theta_{\text{atm}}$, d_s and d_μ . In each panel the undisplayed parameters are integrated out. The “Mixed” and “Restricted” cases correspond to $d_s = 0.5$ and $d_\mu = 0$, respectively.

These limits on the sterile admixture are significantly stronger than obtained previously [11], and play an important role in ruling out four-neutrino oscillation solutions in a combined global analysis of the LSND anomaly [12].

4. Non-standard neutrino interactions

In this section we still focus on atmospheric data, but instead of adding a sterile neutrino we now consider the possibility that neutrinos are massive and moreover possess non-standard interactions with matter [7]. This may be regarded as generic in a large class of theoretical models. For definiteness, in the following we assume that non-standard neutrino interactions occur only with the d -quark. Also, as in Sec. 3 we completely decouple ν_e from atmospheric oscillations. In this case, the propagation of ν_μ and ν_τ inside the Earth is governed by the Hamiltonian:

$$\mathbf{H} = \frac{\Delta m^2_{\text{ATM}}}{4E} \begin{pmatrix} -\cos 2\theta_{\text{ATM}} & \sin 2\theta_{\text{ATM}} \\ \sin 2\theta_{\text{ATM}} & \cos 2\theta_{\text{ATM}} \end{pmatrix} \pm \sqrt{2} G_F N_d(r) \begin{pmatrix} 0 & \varepsilon \\ \varepsilon & \varepsilon' \end{pmatrix}, \quad (3)$$

where the sign + (−) holds for neutrinos (anti-neutrinos), $N_d(r)$ is the number density of the d -quark along the path r of the neutrinos propagating in the Earth, and ε and ε' are phenomenological quantities describing flavor-changing and non-universal non-standard interactions, respectively.

Therefore, as for the sterile neutrino case the transition mechanism depends on four independent parameters. Note that without loss of generality we can restrict the range of the oscillation parameters to $0 \leq \theta_{\text{ATM}} \leq \pi/4$ and $\Delta m^2_{\text{ATM}} \geq 0$, provided that we consider both positive and negative values of the NSI parameters ε and ε' [7]. The details of our analysis are the same as in the previous section.

Our results are summarized in Fig. 3. The global best fit point occurs at $\sin^2(2\theta_{\text{ATM}}) = 1$, $\Delta m^2_{\text{ATM}} = 2.3 \times 10^{-3} \text{ eV}^2$, $\varepsilon = 6.7 \times 10^{-3}$ and $\varepsilon' = \pm 1.1 \times 10^{-3}$. As in the sterile neutrino case, a small component of NSI is preferred, however the effect is not statistically significant: the best pure oscillation solution $\varepsilon = \varepsilon' = 0$, which occurs at $\theta_{\text{ATM}} = 45^\circ$ and $\Delta m^2_{\text{ATM}} = 2.5 \times 10^{-3} \text{ eV}^2$, exhibits a χ^2 which is worse than the global one only by 2.4 units. Thus, the determination of the oscillation parameters Δm^2_{ATM} and θ_{ATM} is stable under the perturbation introduced by the additional NSI mechanism, as can be seen also comparing the “Free” and “Oscillations” lines in the first two panels of Fig. 3. Moreover, the χ^2 function is quite flat in the ε' directions for $\varepsilon' \rightarrow 0$, and almost symmetric under the exchange $\varepsilon' \rightarrow -\varepsilon'$.

On the other hand, the pure NSI solution $\Delta m^2_{\text{ATM}} = 0$ gives a very poor fit, and as already found in Ref. [7] it is completely ruled out. This occurs since the NSI mechanism is not able to reconcile the anomaly observed in the upgoing muon

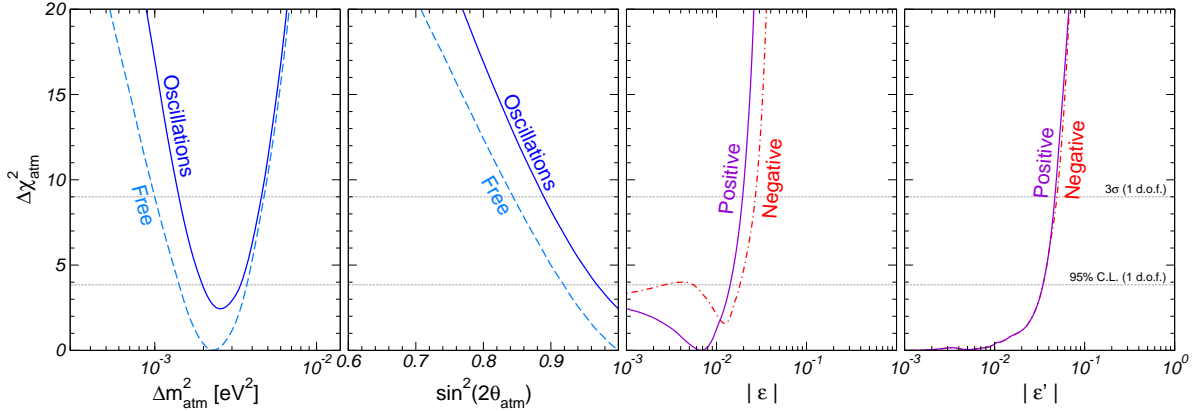


Figure 3. $\Delta\chi_{\text{ATM}}^2$ as a function of Δm_{ATM}^2 , $\sin^2(2\theta_{\text{ATM}})$, $|\varepsilon|$ and $|\varepsilon'|$. The “Oscillations” case corresponds to $\varepsilon = \varepsilon' = 0$. Both “Positive” and “Negative” values of the NSI parameters ε and ε' are displayed.

sample with that seen in the contained event sample. Therefore, when combining the two mechanisms of $\nu_\mu \rightarrow \nu_\tau$ transition, oscillations play the role of leading mechanism, while NSI’s can only be present at a sub-dominant level.

From Fig. 3 we also derive the 3σ allowed ranges: $0.84 \leq \sin^2(2\theta_{\text{ATM}}) \leq 1$ and $1.0 \times 10^{-3} \text{ eV}^2 \leq \Delta m_{\text{ATM}}^2 \leq 4.8 \times 10^{-3} \text{ eV}^2$ for the oscillation parameters, while for the NSI parameters we have $-0.03 \leq \varepsilon \leq 0.02$ and $|\varepsilon'| \leq 0.05$. This is the main result of our analysis, since it provides limits to non-standard neutrino interactions which are truly model independent, being obtained from pure neutrino-physics processes. In particular they do not rely on any relation between neutrinos and charged lepton interactions. Therefore our bounds are totally complementary to what may be derived on the basis of conventional accelerator experiments [18].

5. Conclusions

In this paper we have presented an updated analysis of solar and atmospheric data, both in the context of standard oscillation hypothesis (generalized to account also for a light sterile neutrino), and assuming that neutrino possesses also non-standard interactions with matter.

We have found that both solar and atmospheric neutrino data are very well explained by the simplest hypothesis of oscillations into an active

neutrino, and disfavor the inclusion of an extra sterile state. In fact, at the 3σ level the fraction of sterile neutrino involved in oscillations is limited to be less than 52% in the solar sector and less than 40% in the atmospheric sector. Furthermore, atmospheric data also constrain non-standard neutrino interactions with matter, which are bounded to $-0.03 \leq \varepsilon \leq 0.02$ for the flavor-changing component and $|\varepsilon'| \leq 0.05$ for the non-universal component.

In all the considered cases the determination of the oscillation parameters Δm^2 and θ is stable under the inclusion of exotic physics, such as an extra sterile neutrino or non-standard neutrino-matter interactions. This fact is an evidence in favor of the three-neutrino oscillation solution to the solar and atmospheric neutrino problems. In particular, for what concerns the atmospheric anomaly we conclude that a maximum mixing angle is a solid result, which must be incorporated into any acceptable particle physics model, even in the presence of exotic neutrino interactions.

Acknowledgments

I wish to thank my collaborators N. Fornengo, T. Schwetz, R. Tomàs, M.A. Tórtola and J.W.F. Valle. This work was supported by Spanish grant BFM2002-00345, by the European Commission RTN network HPRN-CT-2000-00148, by the European Science Foundation network grant N. 86

and by the European Union Marie-Curie fellowship HPMF-CT-2000-01008.

REFERENCES

1. M. Shiozawa, talk at Neutrino 2002, <http://neutrino2002.ph.tum.de/>; Y. Fukuda *et al.* [Super-K Coll.], Phys. Rev. Lett. **81** (1998) 1562.
2. A. Surdo, Talk given at *TAUP 2001*, 8–12 September 2001, Gran Sasso, Italy [<http://www.lngs.infn.it/>].
3. Q.R. Ahmad *et al.* [SNO Coll.], Phys. Rev. Lett. **89**, 011301 (2002) [arXiv:nucl-ex/0204008]; Phys. Rev. Lett. **89**, 011302 (2002) [arXiv:nucl-ex/0204009].
4. S. Pakvasa, Pramana **54** (2000) 65 [arXiv:hep-ph/9910246].
5. M. Guzzo *et al.*, Nucl. Phys. B **629** (2002) 479 [arXiv:hep-ph/0112310].
6. M.C. Gonzalez-Garcia and M. Maltoni, arXiv:hep-ph/0202218.
7. N. Fornengo *et al.*, Phys. Rev. D **65** (2002) 013010 [arXiv:hep-ph/0108043].
8. M. Apollonio *et al.* [CHOOZ Coll.], Phys. Lett. B **466** (1999) 415 [arXiv:hep-ex/9907037]; F. Boehm *et al.* [Palo Verde Coll.], Phys. Rev. D **64** (2001) 112001 [arXiv:hep-ex/0107009].
9. C. Athanassopoulos *et al.* [LSND Coll.], Phys. Rev. Lett. **77** (1996) 3082; *ibid.* **81** (1998) 1774; A. Aguilar *et al.* [LSND Coll.], Phys. Rev. D **64** (2001) 112007 [arXiv:hep-ex/0104049].
10. M. Maltoni *et al.*, arXiv:hep-ph/0207227; see also references therein.
11. M. Maltoni, T. Schwetz and J.W.F. Valle, Phys. Rev. D **65** (2002) 093004 [arXiv:hep-ph/0112103].
12. M. Maltoni *et al.*, arXiv:hep-ph/0207157, to appear in Nucl. Phys. B.; see also T. Schwetz, talk at IMFP'2002, to appear in these proceedings.
13. B.T. Cleveland *et al.*, Astrophys. J. **496**, 505 (1998); R. Davis, Prog. Part. Nucl. Phys. **32**, 13 (1994).
14. J.N. Abdurashitov *et al.* [SAGE Coll.], Phys. Rev. C **60**, 055801 (1999); astro-ph/0204245.
15. W. Hampel *et al.* [GALLEX Coll.], Phys. Lett. B **447**, 127 (1999); M. Altmann *et al.* [GNO Coll.], Phys. Lett. B **490** (2000) 16, arXiv:hep-ex/0006034; C. Cattadori *et al.* [GNO Coll.], Nucl. Phys. B (Proc. Suppl.) **110** (2002) 311.
16. M.B. Smy, arXiv:hep-ex/0202020; S. Fukuda *et al.* [Super-K Coll.], Phys. Lett. B **539** (2002) 179 [arXiv:hep-ex/0205075].
17. M.C. Gonzalez-Garcia *et al.*, Phys. Rev. D **63** (2001) 033005 [arXiv:hep-ph/0009350].
18. D. E. Groom *et al.* [Particle Data Group Coll.], Eur. Phys. J. C **15** (2000) 1.